SOILS AND FOUNDATIONS Vol. 21, No. 4, Dec. 1981
Japanese Society of Soil Mechanics and Foundation Engineering

A UNIFIED APPROACH TO THE MODELLING OF LIQUEFACTION AND CYCLIC MOBILITY OF SANDS

ROBERTO NOVA* and TOMASZ HUECKEL**

ABSTRACT

In this paper the problem of liquefaction of sand under either monotonic or cyclic loading is tackled from the point of view of Continuum Mechanics. It is shown that a suitable constitutive model may explain, in a phenomenological sense, the generation of pore pressure in an undrained test either when the load is monotonically increased to failure or when sand is cyclically sheared at constant stress or strain amplitudes. It is demonstrated that in the former case liquefaction of loose samples may be described if a convenient set of constitutive parameters is chosen. It is also shown that liquefaction under cyclic loading may occur even for very dense sands, and that the essential features revealed by experiments, such as progressive pore pressure build-up accompanied by small shear strains followed by a sudden pore pressure increase with large strains, are correctly modelled by the theory.

The constitutive model employed is a combination of a classical elastoplastic constitutive law, which proved to be successful in modelling the behaviour of sand under monotonic loading, and of a law allowing for hysteresis, which applies to loading processes within the yield locus, especially conceived to interpret the behaviour of soils under cyclic loading.

Key words : constitutive relations, cyclic mobility, liquefaction, plasticity, triaxial tests, unloading-reloading
IGC : D 6/D 7

INTRODUCTION

This paper is concerned with the mathematical modelling of the development of high pore water pressure in saturated sands in undrained conditions.. This phenomenon is believed to be the primary cause of several flow slides and of catastrophic sinking of footings supported on sand during earthquakes. It may be observed in laboratory either for monotonically loaded samples of loose contractive sands or for specimens of both loose and dense sands under cyclic loading.

As a consequence of the increase of the pore water pressure the shear strength of sand is reduced, since the neutral pressure tends to reach the value of the confining stress in the triaxial cell. This extreme condition has been called liquefaction by different authors, irrespectively of the way in which it is achieved. In reality, however, this phenomenon, when considered from the point of view of Continuum Mechanics, has completely different explanations depending whether it is due to monotonic or cyclic loading. In fact, such a

* Department of Structural Engineering, Technical University of Milano, Italy.
** Institute of Fundamental Technological Research, IPPT/PAN, Warsaw, Poland.
Written discussions on this paper should be submitted before October 1, 1982.

distinction has been forwarded by Casagrande e. g. (1975) and Castro (1975). Castro proposed a possible classification distinguishing the phenomenon of "liquefaction" (or "actual liquefaction" as suggested by Casagrande) from the phenomenon of "cyclic mobility" (or "cyclic liquefaction" following Casagrande).

The two definitions refer to situations that can be summarized as follows.

Liquefaction may occur in loose saturated sand subjected to *monotonic* loading in undrained conditions. It denotes a state in which, due to the pore pressure increase, the effective isotropic stress drops to a very low value together with the shear strength. The sand may be then sheared to large strains at a constant, very low, shear stress, as if it were a fluid.

Cyclic mobility denotes the phenomenon which consists in the development of high pore pressure under *cyclic* loading in undrained conditions. The sand reaches a liquefied state when the effective isotropic pressure approaches zero. At variance with the liquefaction induced by static loading this happens only momentarily and it may occur even in very dense sands if sheared for a sufficient number of cycles. However, only loose specimens undergo large strains under further loading, whilst dense samples develop only moderate strains.

The aim of this paper is to show that each of the two phenomena has different mechanical origin, but that both may be qualitatively and quantitatively described within the framework of a suitable constitutive mathematical model, based on the concept of strain-hardening elastoplasticity with account of hysteresis in unloading and reloading.

The constitutive law that will be used herein is a slight modification of that already formulated by the authors (Nova and Hueckel, 1979, 1980). It is composed of two parts. The former which applies to virgin loading is a generalization to three-dimensional loadings of the model by Nova and Wood (1979), and is a classical elastic-plastic constitutive law allowing for hardening and softening in the same spirit of the Cam Clay model (Schofield and Wroth, 1968 ; Roscoe and Burland, 1968). The latter part, which applies to the behaviour of soil under unloading and reloading, within the yield locus defined by the former law, is piecewise path independent. To make this paper self-contained a short outline of this model will be given in section 2 and section 4.

OUTLINES OF THE ELASTIC-PLASTIC CONSTITUTIVE LAW

For the sake of simplicity only triaxial tests will be considered, and the constitutive law will be written in terms of "triaxial" stresses and strains ; i. e. the mean effective stress p', the deviatoric stress q, the volumetric strain v and the deviatoric strain ε defined as follows

$$\left.\begin{array}{ll} p'=(\sigma_a'+2\sigma_r')/3\,; & q=\sigma_a-\sigma_r \\ v=\varepsilon_a+2\varepsilon_r & \varepsilon=2/3(\varepsilon_a-\varepsilon_r) \end{array}\right\} \qquad (1)$$

Indices a and r mean axial and radial, respectively. Stress and strain are taken as positive in compression. A superscript p or e will indicate plastic or elastic strains respectively, a dot will indicate increment or rate, a dash effective stress. A three-dimensional generalization of the constitutive law involving tensorial notation has been given in Nova and Hueckel (1980).

Consider first a specimen of sand prepared in the laboratory either in a dense or in a loose state. It is well known that under a cycle of loading and subsequent unloading, even at very low stress amplitude, the specimen exhibits some irrecoverable strain even in purely isotropic loading conditions. Thus the behaviour of the material can be treated as elastoplastic since the very beginning of the loading process and it is possible to assume that, initially, the purely elastic range does not exist.

Strain rates may be splitted into an elastic (recoverable) and plastic (irrecoverable) part, so that

$$\dot{v}=\dot{v}^e+\dot{v}^p\ ;\quad \dot{\varepsilon}=\dot{\varepsilon}^e+\dot{\varepsilon}^p \tag{2}$$

To determine the strain response of the material to a given stress it is necessary to specify the elastic and plastic parts of the incremental law. The latter is defined through a yield function $f=f(p',q',\psi)$, a hardening parameter $\psi=\psi(v^p,\varepsilon^p)$ and a plastic potential $g=g(p',q)$. The plastic potential is an auxiliary function which makes it possible to write the plastic strain rates as

$$\dot{v}^p=\Lambda\partial g/\partial p'\ ;\quad \dot{\varepsilon}^p=\Lambda\partial g/\partial q \tag{3}$$

Thus the vector of the plastic strain rates $(\dot{v}^p,\dot{\varepsilon}^p)$ is directed along the gradient of the potential $g=g(p',q)$. The proportionality parameter Λ indicates that the modulus of the plastic strain rate vector is proportional to the stress rate projection onto the yield function gradient and is inversely proportional to a hardening modulus $H=H(\psi,p',q)$ so that :

$$\Lambda=\frac{\partial f/\partial p'\cdot\dot{p}'+\partial f/\partial q\cdot\dot{q}}{H} \tag{4}$$

where the plastic hardening modulus H is equal to

$$H=-\partial f/\partial\psi(\partial\psi/\partial v^p\cdot\partial g/\partial p'+\partial\psi/\partial\varepsilon^p\cdot\partial g/\partial q) \tag{5}$$

Relations (4) and (5) can be derived simply by noting that plastic strains occur only when the stress point lies on the current yield surface i. e.

$$f=0\ ;\quad \dot{f}=\partial f/\partial p'\cdot\dot{p}'+\partial f/\partial q\cdot\dot{q}+\partial f/\partial\psi\cdot\dot{\psi}=0 \tag{6}$$

The hardening modulus may be either positive or negative or zero, corresponding to hardening, softening or perfectly plastic (critical state) behaviour, respectively. The parameter Λ is positive at plastic yielding, i. e. if (6) is verified, and is zero otherwise. The explicit forms of the functions, f, g, ψ, which will be employed in the following have been derived from analyses of experimental data on sand and are discussed in Nova, Wood (1979). They may be formulated as follows.

$$f=4\mu\eta^2/M^2+1-(p_c'/p')^2=0\ ;\quad \eta\leq M/2 \tag{7}$$

$$f=\eta/M+m/M\ln(p'/p_y')-1=0\ ;\quad \eta\geq M/2 \tag{8}$$

$$g=f\ ;\quad \eta\leq M/2 \tag{9}$$

$$g=\eta/M\cdot(1-\mu)-(1-\mu(p'/p_g')^{1-\mu/\mu})=0\ ;\quad \eta\geq M/2 \tag{10}$$

$$\psi=p_c'\ ;\quad p_y'=Yp_c'\ ;\quad p_g'=Zp_c' \tag{11}$$

$$p_c'=\exp(1/(\lambda-B_0)\cdot(v^p+D\varepsilon^p))-1 \tag{12}$$

The variable η is called stress ratio and is defined as

$$\eta\equiv q/p' \tag{13}$$

The parameters m, μ, M, λ, B_0 and D are material constants, while p_c' is the abscissa of the yield curve at $\eta=0$, i. e. the preconsolidation pressure, p_y' is the abscissa at $\eta=M$ and p_g' is the abscissa of the plastic potential curve at $\eta=M$, as shown in Figs. 1, 2. The parameter M is the stress ratio for which the plastic dilatancy $d\equiv\dot{v}^p/\dot{\varepsilon}^p$ is zero. It appears then to be the critical state stress ratio, as defined in Cam Clay. The proportionality constants Y, Z may be easily derived from the Eqs. (7)-(10).

The elastic strain rates in an elastic-plastic process may be assumed to be

$$\dot{v}^e=B_0\cdot\dot{p}'/p'\ ;\quad \dot{\varepsilon}^e=2/3\,L_0\dot{\eta} \tag{14}$$

This relation can be viewed as a sort of Hooke law in terms of so called 'geotechnical

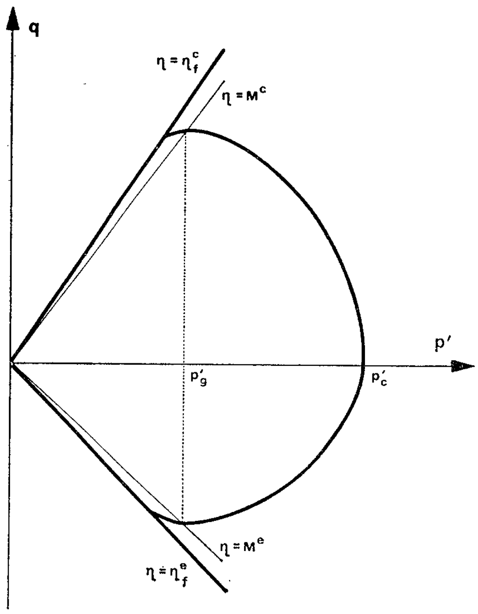

Fig. 1. The plastic potential

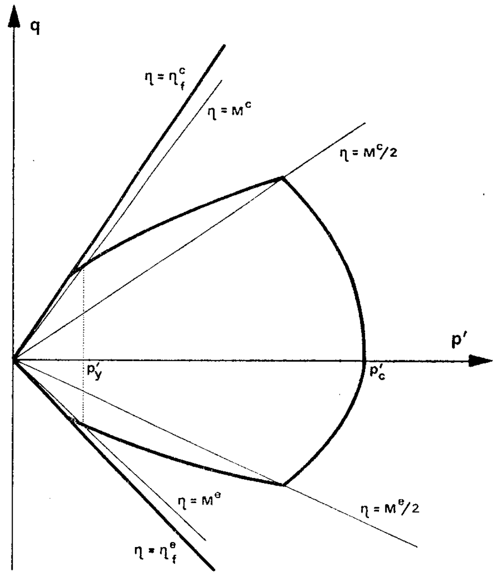

Fig. 2. The yield locus

stress variables' (Nova and Hueckel, 1980) which proved to be very useful in simplifying both the interpretation and the description of the highly non-linear behaviour of soil.

The total incremental strain takes thus the following form

$$\dot{v}=B_0\cdot\dot{p}'/p'+\Lambda d\ ;\ \dot{\varepsilon}=2/3\,L_0\dot{\eta}+\Lambda, \tag{15}$$

where

$$\Lambda=(\lambda-B_0)\frac{(d+\eta)\dot{p}'/p'+\dot{\eta}}{(d+\eta)(d+D)}\quad\text{and}\quad d=M^2/(4\mu\eta)\ ;\quad \eta\leq M/2 \tag{16}$$

$$\Lambda=(\lambda-B_0)\frac{m\dot{p}'/p'+\dot{\eta}}{m(d+D)}\ \text{and}\quad d=(M-\eta)/\mu\ ;\quad \eta\geq M/2 \tag{17}$$

By integrating Eq. (15) it is possible to determine the complete strain history of the sample for a given stress path. This gives reasonable results in many conventional compression tests, as shown by Nova and Wood (1979). Note that the model predicts that the critical state line and the line of phase transformation, as defined by Ishihara, Tatsuoka and Yasuda (1975), coincide, as it is apparent from Eqs. (15) and (17).

As it is well known, the behaviour of soils, under a given cell pressure, is different depending whether the stress deviator, as defined in Eq. (1), is positive or negative, i. e. whether the soil is under 'compression' or under 'extension'. However the behaviour is qualitatively similar. This suggests that the structure of the equations governing the behaviour in 'compression' and 'extenstion' is the same although the constitutive parameters are different. It is found to be a suitable assumption to set the ratios m/M and D/M equal in 'compression' and in 'extension' ranges, whilst M is different. Indeed Eqs. (15) are conceived in such a way that, after integration, the parameters m and D appear always normalized with respect to M. The critical stress ratios M^c and M^e are thus defined as follows, assuming that the angle of internal friction at constant volume (for large strains) ϕ_{cv}' is a fundamental material characteristic, independent of the sign of the stress deviator :

$$M=M^c=6\sin\phi_{cv}'/(3-\sin\phi_{cv}')\ \text{ in 'compression' }(q>0) \tag{18}$$

$$M=M^e=6\sin\phi_{cv}'/(3+\sin\phi_{cv}')\ \text{ in 'extension' }(q<0) \tag{19}$$

On the other hand, however, it is well known that the peak angle of friction in an undrained extension test is in general different from the corresponding angle in compression. This may be taken into account in the following way. Nova and Wood (1979) assumed that the peak angle of friction in a drained test is equal to the limiting angle of friction in an undrained test on loose sand. This implies that the maximum achievable stress ratio in compression is given by

$$\eta_f{}^c = M^c(1 + B_0/\lambda \cdot \mu \cdot D^c/M^c) \tag{20}$$

Assuming that B_0, λ and μ are the same in the two cases, what seems reasonable because λ and B_0 are derived in an isotropic test and μ appears as a non-normalized variable in the stress-strain relations, it is possible to find

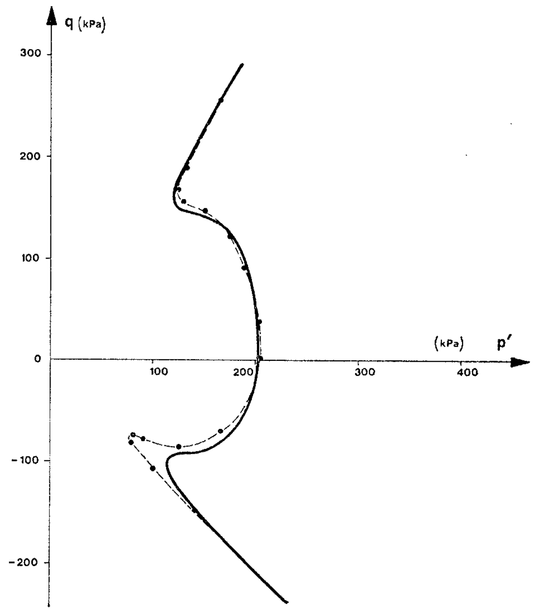

(a) Stress paths

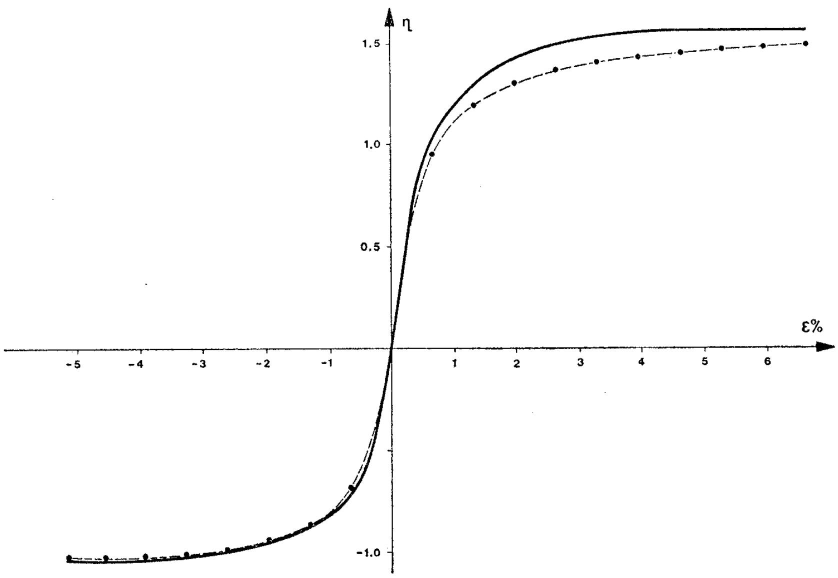

(b) Shear strains

Fig. 3. Comparison between calculated and experimental results in undrained compression and extension tests on loose Fuji River sand-data from Tatsuoka (1972)

$$\eta_f{}^e = M^e(1+B_0/\lambda\cdot\mu\cdot D^e/M^e) = \eta_f{}^c M^e/M^c \tag{21}$$

since

$$D^e/M^e = D^c/M^c = D/M \tag{22}$$

It is easy to show that to $\eta_f{}^c$ and $\eta_f{}^e$ correspond two different friction angles ϕ'^c, ϕ'^e and that the latter is larger, since

$$\frac{\sin\phi_c'}{\sin\phi_e'} = \frac{3-\sin\phi_{cv}'\cdot(B_0/\lambda\cdot\mu\cdot D/M)}{3+\sin\phi_{cv}'\cdot(B_0/\lambda\cdot\mu\cdot D/M)}$$

In Fig. 3 the stress paths and the stress curves in two undrained tests in compression and in extension are compared with experimental findings-data from Tatsuoka (1972). Note that the constitutive parameters are those employed by Nova and Wood (1979) to interpret a set of compression tests performed by the same researcher. They are $M^c=1.34$, $m/M=.41$, $D/M=.419$, $B_0=.00544$, $\lambda=.01275$, $L_0=.00715$, $\mu=.7$.

Following this way of reasoning it is formally possible to extend the expression of the constitutive relations to general poliaxial loading conditions via the parameter $b\equiv(\sigma_2-\sigma_3)/(\sigma_1-\sigma_3)$.

LIQUEFACTION OF SAND UNDER MONOTONIC LOADING

Consider an undrained test. Integrating the Eqs. (15) under the condition of constant volume it is possible to find the closed form solution for the effective stress path as follows :

$0\leq\eta\leq M/2$:

$$\ln(p'/p_c) = \frac{1-B_0/\lambda}{1+D^2/a\cdot B_0{}^2/\lambda^2}\left[\frac{1}{2}\ln(1+\eta^2/a) + B_0D/\lambda\sqrt{a}\cdot\tan^{-1}(\eta/\sqrt{a}) - \ln(1+B_0/\lambda\cdot D/(a\cdot\eta))\right];$$

$$a\equiv M^2/4\mu \tag{23}$$

$M/2\leq\eta$

$$\ln(p'/p_c) = (\ln p'/p_c)_{\eta=M/2} - \frac{1-B_0/\lambda}{m/M}\cdot\left[\eta/M-\frac{1}{2}+B_0/\lambda\cdot D/M\cdot\mu\cdot\ln\left(1+\frac{\frac{1}{2}-\eta/M}{\frac{1}{2}+\frac{B_0D\mu}{\lambda M}}\right)\right] \tag{24}$$

The shape of the stress path is given in Fig. 4 for different values of D/M. It is visualized that the stress path may take different forms depending on this ratio. In fact, it has been shown (Nova, 1980) that if

$$D/M<(D/M)_{\mathrm{crit}}\equiv 1/\mu\frac{(1-m/M-B_0/\lambda)^2}{4(1-B_0/\lambda)\mu B_0/(\lambda M)} \tag{25}$$

the stress path in the (q, p') plane has a local maximum and a local minimum. Thus in a load controlled test the deviatoric stress reaches a peak after which it decreases although the axial load remains constant since the area of the cross section of the specimen increases rapidly. This process is associated with a large increase of the pore pressure. However, after a while, the decrease of q is arrested at a local minimum of the stress path and, in the following the deviatoric stress increases again, accompanied first by a further limited drop of the effective pressure and finally by its remarkable increase, so that the stress path asymptotically approaches the failure line. This latter phase of the process is con-

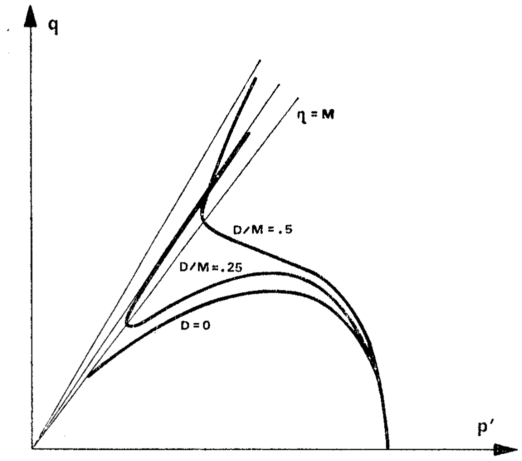

Fig. 4. Calculated stress paths for different values of *D/M*

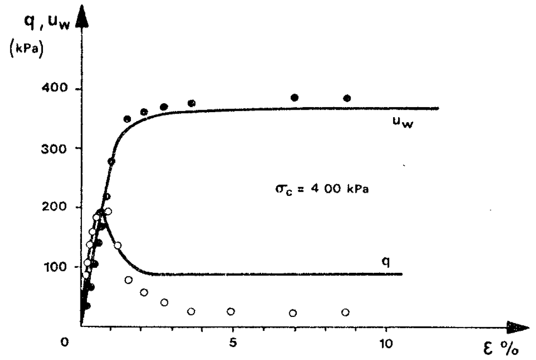

Fig. 5. Comparison between calculated and experimental results in undrained monotonic loading on loose Banding sand-data after Castro (1969)

nected with a decrease of the pore water pressure. Such phenomenon has been experimentally observed and called by Casagrande 'partial liquefaction'.

If the value of D is very small (in the limiting case equal to zero) it may occur, for a suitable combination of the other constitutive parameters, that the deviatoric stress reaches its minimum (which is a very low value) in the presence of large strain. Correspondingly the pore pressure approaches the total confining pressure and the isotropic effective stress is practically equal to zero. This phenomenon is called by Casagrande 'actual liquefaction'. For both cases it is possible to derive the deviatoric stress–strain relation once the equation of the stress path is known. In Fig. 5 the comparison is presented between the experimental results obtained by Castro (1969) and the results calculated for $M^c=1.2$, $\lambda=.00807$, $B^0=.00151$, $L_0=.00818$, $\mu=1$, $m/M=.292$, $D/M=0$. It can be seen that the agreement is rather satisfactory. It can be also deduced from the equation of the stress path (24) that if

$$D/M \geq (D/M)_{crit} \tag{26}$$

the effective stress path in the q, p' plane has no extrema and thus neither partial nor actual liquefaction may occur.

The constitutive parameters are assumed to depend on the *initial* void ratio, i. e. the void ratio after deposition, but not on the consolidation pressure, at least for moderate stress ranges. This implies that the undrained stress path at different cell pressures are all given by the same equation in terms of η and ln (p'/p'_c), what results in stress paths of the same shape in the (q, p') plane. This seems to be experimentally verified, at least for not very low confining pressures, see e. g. Tatsuoka (1972). On the other hand, the void ratio decreases roughly logarithmically, with the increasing consolidation pressure.

Since ϕ_{cv}' for a given sand does not depend on its density, so does not M^c. The parameters B_0, λ, μ are also not markedly influenced by the porosity of the sand, whilst D increases with decreasing initial void ratio. The looser specimens are characterized by values of D/M that are lower than the critical value, $(D/M)_{crit}$. Therefore for such a specimen (I) at least partial liquefaction will occur. This sample may be densified by increasing the confining pressure. But since D does not vary, partial liquefaction will occur any way. Two different states are shown to belong to the isotropic consolidation line $A-B$ in the Fig. 6. Another sample (II), initially denser than (I), can be conceived so that its value of D/M is higher than $(D/M)_{crit}$, point C, Fig. 6, and then liquefaction can never be achieved. Thus if the sample is brought to the void ratio e_B by increasing

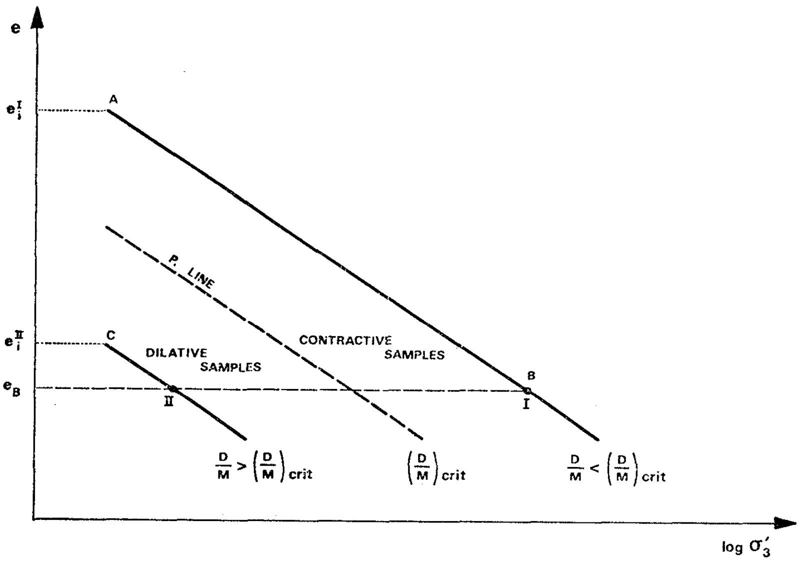

Fig. 6. State diagram. The *P* line delineates between samples of a given sand which will (contractive) or will not (dilative) undergo at least partial liquefaction. States refer to condition *before* undrained loading

the confining pressure, there are two samples (I) and (II) at the same void ratio, but different confining pressures and different susceptibility to liquefaction. In this way a family of lines can be defined in the plane (e, σ_3') each one associated with a particular value of D/M. The one corresponding to $D/M=(D/M)_{crit}$ discriminates between the liquefiable and non liquefiable states and corresponds to Castro's (1969) P line.

Thus the well-known state diagram for liquefaction can be conceptually reproduced by means of the mathematical model discussed.

Note that $(D/M)_{crit}$ depends on the value of the other constitutive parameters. They in turn depend on the internal structure of the considered sand and indirectly reflect the properties of the sand deposit, such as age, roundness and dimensions of particles, uniformity coefficient and mineralogy. The experimental finding that a certain type of sand is more or less susceptible to liquefaction is then indirectly taken into account by the numerical values of the constitutive parameters.

From the results discussed in this section it is then evident that the phenomenon of liquefaction of sand under monotonic undrained loading may be described within the same framework that allows to model the behaviour of sand in the common drained or undrained laboratory tests.

Finally, a reasonable estimate of the post-peak behaviour is possible via a simple analysis of the dynamic equilibrium of the sample, as shown in the Appendix.

THE CONSTITUTIVE LAW FOR UNLOADING AND RELOADING

In order to describe cyclic mobility of sand, the response to a generic stress path within the yield locus should be suitably interpreted and mathematically formulated. The behaviour in unloading and reloading can not be successfully described by an elastic-constitutive law, even if nonlinear. Indeed, the phenomena of histeresis and cyclic compaction, which are believed to be crucial in the description of cyclic mobility, are absent in the elastic description because of its very nature of total reversibility.

The model that will be presented below is a slight modification of the one developed by the authors (Hueckel and Nova, 1979 ; Nova and Hueckel, 1980). It is based on the hypothesis that the behaviour within the current yield locus and the elastoplastic behaviour do not affect each other. Moreover it is assumed that the loading path within the yield locus may be divided into well defined portions each of which may be considered separately. Every portion originates at a stress point at which drastic changes in stress rate direction occur. These points will be called henceforth stress reversal points, following a definition given by Mroz and Lind (1975). Their rigorous definition will be given later on. The behaviour between two stress reversal points is thought to be independent of the previous material history except for what concerns the values of the compliance moduli at the onset of the portion. Moreover it is supposed to be independent of the path followed from the origin of the current portion to the current state. Therefore such a behaviour has been called "piecewisely path independent" and strains developed during such a process 'paraelastic strains'.

In the triaxial plane the piecewise path independent constitutive law has been formulated as follows :

$$^{\Delta L}v=B\ln\frac{p'}{p'_L}+\xi^{*\Delta L}\chi=B_0(1+\omega_v{}^{\Delta L}\chi)\ln\frac{p'}{p'_L}+\xi^{*\Delta L}\chi \tag{27}$$

$$^{\Delta L}\varepsilon=\frac{2}{3}L^{\Delta L}\eta=\frac{2}{3}L_0(1+\omega_\varepsilon{}^{\Delta L}\chi)^{\Delta L}\eta \tag{28}$$

where B, L and B_0, L_0 are the current and initial bulk and deviatoric compliance moduli, respectively, ω_v and ω_ε are constants. The value $^{\Delta L}\chi$ is called strain amplitude after Hardin and Drnevich (1972) and is defined as follows :

$$^{\Delta L}\chi=(1/3\,{}^{\Delta L}v^2+3/2\,{}^{\Delta L}\varepsilon^2)^{1/2} \tag{29}$$

All quantities preceded by a prefix $^{\Delta L}$ are referred to the L-th point, in order of occurrence, at which the last stress reversal took place. Thus the law (27)-(28) is written in terms of differences between the current value of a quantity and its value at the point L, i. e.

$$^{\Delta L}x=x-x^L \tag{30}$$

The non-negative term ξ^* will be called cumulative strains modulus. When it is equal to zero, the constitutive law (27)-(30) implies the existence in radial paths of a polar symmetry of any closed unloading-reloading loop in the space of the strain components $^{\Delta L}v$, $^{\Delta L}\varepsilon$ and the so called 'geotechnical' stress variables ($\ln p'/p'_L$, $^{\Delta L}\eta$).

The state characterized by $\xi^*=0$ is conceived to correspond to the stabilization of the stress-strain loop, what may occur after a certain number of cycles. From (27)-(28) it is seen that due to the presence of the term $\xi^{*\Delta L}\chi$ and to its positiveness, a cumulation of volumetric strains occur during cyclic loading.

The cumulative strain modulus ξ^* is defined as follows

$$\xi^*=\xi\Big/\Big(\chi^p+\sum_{1}^{L}{}_i\,({}^{\Delta i}\chi-{}^{\Delta i}\chi^e)\Big) \tag{31}$$

Where ξ is a material constant, χ^p is the plastic strain amplitude

$$\chi^p=(1/3\,v^{p2}+3/2\,\varepsilon^{p2})^{1/2} \tag{32}$$

The term $({}^{\Delta i}\chi-{}^{\Delta i}\chi^e)$ has the sense of a cumulative strain amplitude over the i-th portion of the material hysteretic history, since $^{\Delta L}\chi^e$ is defined as

$$^{\Delta i}\chi^e=(1/3(B_0\ln p'/p'_i)^2+3/2(2/3\,L_0{}^{\Delta i}\eta)^2)^{1/2} \tag{33}$$

Therefore the denominator of (31) is the sum of the irreversible strain amplitudes experienced by the material during its history. It has the following properties : it is constant over a single portion of material history ; it encompasses the previous plastic strains (for example the consolidation strains) ; within a given yield locus it makes ξ^* to decrease at each subsequent stress reversal (or semi-cycle) so that it may even asymptotically vanish, if the number of cycles is high enough.

The definition of stress reversal point whose meaning is straight-forward in the case of radial loading programmes, require a more sophisticated formulation in pluriaxial conditions. A stress increment (or rate) gives rise to the $L+1$-th reversal if, in a given point, it reenters a stress locus $W-W_0=0$, of constant strain amplitude, defined as follows

$$W-W_0={}^{\Delta L}\chi^2(\eta,\ \ln p'/p_L)-W_0=(B\ln p'/p_L+\xi^{*\Delta L}\chi)^2+(2/3\,L^{\Delta L}\eta)^2-W_0=0 \tag{34}$$

In terms of the 'geotechnical' variables $\ln p'/p_L$, ${}^{\Delta L}\eta$, the locus is an ellipse. Its center moves along the hydrostatic pressure axis as ${}^{\Delta L}\chi$ increases, starting from the L-th stress reversal point. The axes of the ellipse are coincident with the coordinate system and grow, not necessarily proportionally, with ${}^{\Delta L}\chi$.

Thus if the stress rate increment vector $(\dot{\eta},\ \dot{p}'/p')$ is such that

$$\mathcal{L}=\partial W/\partial(\ln p'/p_L)\cdot\dot{p}'/p'+\partial W/\partial({}^{\Delta L}\eta)\dot{\eta}<0 \tag{35}$$

the $(L+1)$th reversal occurs and begins a new portion of the material history, described as independent of the previous ones, except for the initial characteristics, B_0, L_0, ξ^*.

If the stress rate is such that $\mathcal{L}>0$, the current L-th law continues to be valid, whilst if $\mathcal{L}=0$, both laws give an identical incremental response. The latter case is assessed via a discrete dependence of B_0 and L_0 on the $(\dot{\eta},\ \dot{p}'/p')$ vector at the reversal, so that it complies with the requirement of total compliance restoration for perfect reversal (in terms of its direction) and of compliance continuity for $\mathcal{L}=0$. More details and generalization to the multidimensional tensorial formulation together with more complex path memory effects may be found in Hueckel and Nova (1979), Nova and Hueckel (1980) and Hueckel (1981).

It is interesting to relate the present formulation to the results elaborated in the framework of the approach by Hardin and Drnevich (1972) in which the soil behaviour is characterized by a variable (secant) shear modulus and a damping ratio R_D. Consider then a p' constant test, that is conceptually similar to the hollow cylinder test performed by the quoted authors. If the soil is virgin, i. e. normally consolidated, the first loading necessarily produces elastoplastic strains and may be modelled by an elastic-plastic constitutive law. Further unloading-reloading occurs within the current yield locus. Then for a semi-cycle, Eq. (27) gives

$${}^{\Delta L}v=\xi^*(1/3\,{}^{\Delta L}v^2+3/2\,{}^{\Delta L}\varepsilon^2)^{1/2} \tag{36}$$

The constant ξ^* according to its definition (31) has to be evaluated at the onset of the semi-cycle. From (36) the ratio between strain differences can be found as

$${}^{\Delta L}v=(3/2\,\xi^{*2}/(1-\xi^{*2}/3))^{1/2}|\Delta\varepsilon|\,. \tag{37}$$

The volumetric strains are thus always positive (compaction). Through (37), (29) and (28) the equation for the single semi-cycle reads

$${}^{\Delta L}\varepsilon=\frac{2/3\,L_0\cdot{}^{\Delta L}q/p'}{1-(2/(3\cdot(1-\xi^{*2}/3)))^{1/2}L_0\omega_s\cdot|{}^{\Delta L}q/p'|} \tag{38}$$

The secant shear modulus in this test thus becomes

$$G=\frac{{}^{\Delta L}q}{{}^{\Delta L}\varepsilon}=\frac{p'}{2/3\,L_0(1+\sqrt{3/2(1-\xi^{*2}/3)}\,\omega_s|{}^{\Delta L}\varepsilon|)} \tag{39}$$

It may be seen that for a single loop the shear modulus G decreases with increasing $\Delta\varepsilon$, ds shown in Fig. 7, in a way similar to that experimentally observed, see e. g. Hardin and Drnevich (1972).

The damping ratio is defined as

$$R_D=A_L/(4\pi A_T) \tag{40}$$

where A_L and A_T are the area of the loop and the hatched area in Fig. 8(a), respectively. The latter represents a fictitious elastic strain energy pertinent to the secant modulus G. These definitions rest on the assumption of perfect closure of the loops and therefore, for the sake of comparison, we shall neglect the term of cyclic compaction by setting $\xi^*=0$.

Thus the damping ratio takes the form

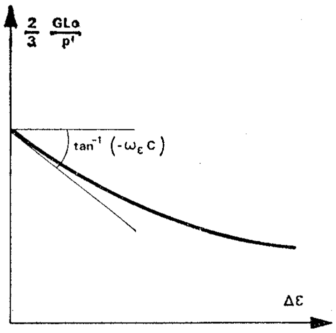

Fig. 7. Variation of shear modulus with shear strain amplitude

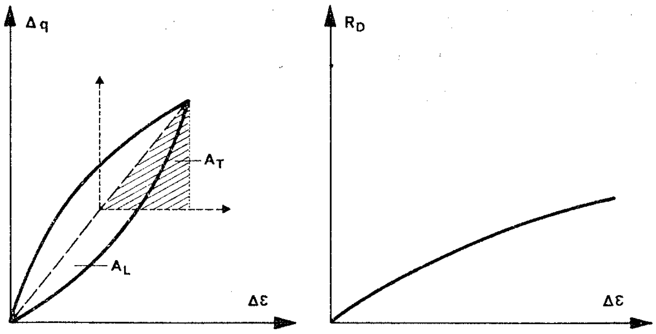

(a) (b)

Fig. 8. Definition of damping ratio and its variation with shear strain amplitude

$$R_D=2/\pi\left\{1+\frac{2}{\sqrt{3/2}\,\omega_\varepsilon{}^{\Delta L}\varepsilon}-\frac{2(1+\sqrt{3/2}\,\omega_\varepsilon{}^{\Delta L}\varepsilon\ \ln\,(1+\sqrt{3/2}\,\omega_\varepsilon{}^{\Delta L}\varepsilon))}{(\sqrt{3/2}\,\omega_\varepsilon{}^{\Delta L}\varepsilon)^2}\right\} \tag{41}$$

The variation of R_D with ${}^{\Delta L}\varepsilon$ is given in Fig. 8(b). The qualitative agreement with experimental findings seems satisfactory.

Finally it is worth noting that, if a constant volume test is performed, if the cumulative strain modulus ξ^* is non-zero, changes in isotropic pressure are to be expected, as can be seen from Eq. (27). This effect is of fundamental importance for further considerations that will be carried on in sec. 5.

THE MODELLING OF CYCLIC MOBILITY

It is now possible to model even the phenomenon of liquefaction under cyclic loading. Consider for example a stress controlled test like that of Fig. 9 reported by Ishihara, Tatsuoka and Yasuda (1975). The cycling starts with an extension phase and is followed by a compression. The effective stress point moves leftward with relatively small deformations, untill large strains are developed and the pore pressure rises practically to the value of the confining pressure, so that liquefaction occurs.

The first extension phase may be modelled by the elastic plastic constitutive law. The stress path is given by Eq. (23). Since the sand employed by the quoted authors is apparently the same used by Tatsuoka (1972) to which Figs. 3(a) and 3(b) refer, the constitutive parameters concerning the elastoplastic phase are those already used in section 2. Note that those parameters have been firstly derived to model compression tests.

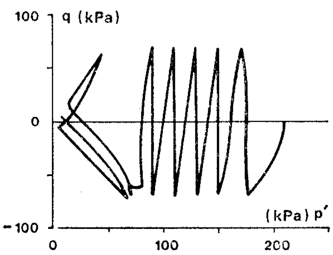

Fig. 9. Cyclic stress controlled test. After Ishihara, Tatsuoka and Yasuda (1975)

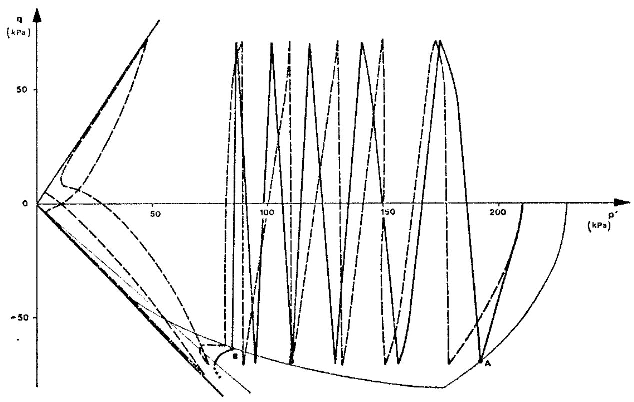

Fig. 10. Comparison between calculated and experimental stress paths of Fig. 9

At point A the first stress reversal occurs. The yield locus passing through A is given by the thin curve shown in Fig. 10. For further loading the paraelastic model applies. Since ξ^* is constant for a single branch and the undrained condition implies ${}^{\Delta L}v=0$,

$$B_0 \ln p'/p_L(1+\omega_v\chi)+\xi^*\chi=0 \tag{42}$$

from which

$$p'=p_L \exp\,(\xi^*\chi/B_0(1+\omega_v\chi)) \tag{43}$$

since

$$\chi=\sqrt{3/2}\,|\Delta\varepsilon|=\frac{\sqrt{2/3}\,L_0|\Delta\eta|}{1-\omega_\varepsilon\sqrt{2/3}\,L_0|\Delta\eta|} \tag{44}$$

the stress path is easily determined. By choosing suitable constitutive parameters, namely $\xi=.00065$, $\omega_v=20.0$, $\omega_\varepsilon=30.0$, it is possible to derive a stress path which very well simulates the actual behaviour of the sand. Shear strains increase with increasing ${}^{\Delta L}\eta$ but in the hysteretic domain are not greater than 1.3% which are larger than the measured but still very small.

At point B the yield locus is reached and the elasto-plastic model must be employed to describe further loading. From Eq. (24) it is possible to derive the stress path equation, that is

$$\ln p'/p_i'=\frac{1-B_0/\lambda}{m/M}\left[\eta/M^e-\eta_i/M^e+B_0D/\lambda M\mu \ln\left(1+\frac{\eta_i/M^e-\eta/M^e}{1-\eta^i/M^e+\dfrac{B_0D}{\lambda M}}\right)\right] \tag{45}$$

The calculated stress path changes abruptly direction, reaches rapidly the $\eta=M^e$ line and performs a hook around this line as experimentally observed. Strains increase dramatically and become of the order of 20% and more, in accordance with the experimental findings.

From this point the incremental modelling of the behaviour has very little meaning. First of all the hypothesis of small strains on which most of the constitutive models available in the literature rests is macroscopically violated. Moreover Casagrande (1975) has shown that cyclic mobility produces a redistribution of water content within the specimen that cannot be considered uniform anymore. It is interesting however to note that the experimental stress path approaches, after liquefaction, the lines

$$\eta_f{}^c=M^c(1+B_0/\lambda\cdot D/M\cdot\mu)$$

$$\eta_f{}^e=M^e(1+B_0/\lambda\cdot D/M\cdot\mu)$$

which are lines for which $\dot{v}=0$ in the elastoplastic domain.

Another test that may be modelled is a cyclic undrained test at constant shear strain amplitude, such as that reported by Ishihara Tatsuoka and Yasuda, shown in Fig. 11(a). The calculated stress path is shown in Fig. 11(b). In the paraelastic range, an undrained constant strain amplitude test implies constant $\Delta\eta$-see Eq. (28). It can be seen that this is approximately what is observed in experiments. However to get in calculations the same $\Delta\eta$ as in experiment the value of the deviatoric strain amplitude must be of 0.912% instead of 0.44%, used by the quoted authors.

Consider finally a cyclic stress controlled compression test on a loose specimen of the same sand which exhibited liquefaction under monotonic loading. Using the same parameters employed to model loose Banding sand, combined for the sake of convenience with the hysteretic parameters used for Fuji River sand, it is possible to get a reasonable trend of the stress path, as shown in Fig. 12(b), that reflects the essential features of that found by Castro (1969) in such kind of tests on loose Banding sand and shown in Fig. 12(a). Note that the pore pressure reaches the 90% of the value of the confining pressure. Strains are small until point A, where the yield locus is reached, and tend theoretically to infinity in the portion AB. The point A corresponds to a local maximum of the shear

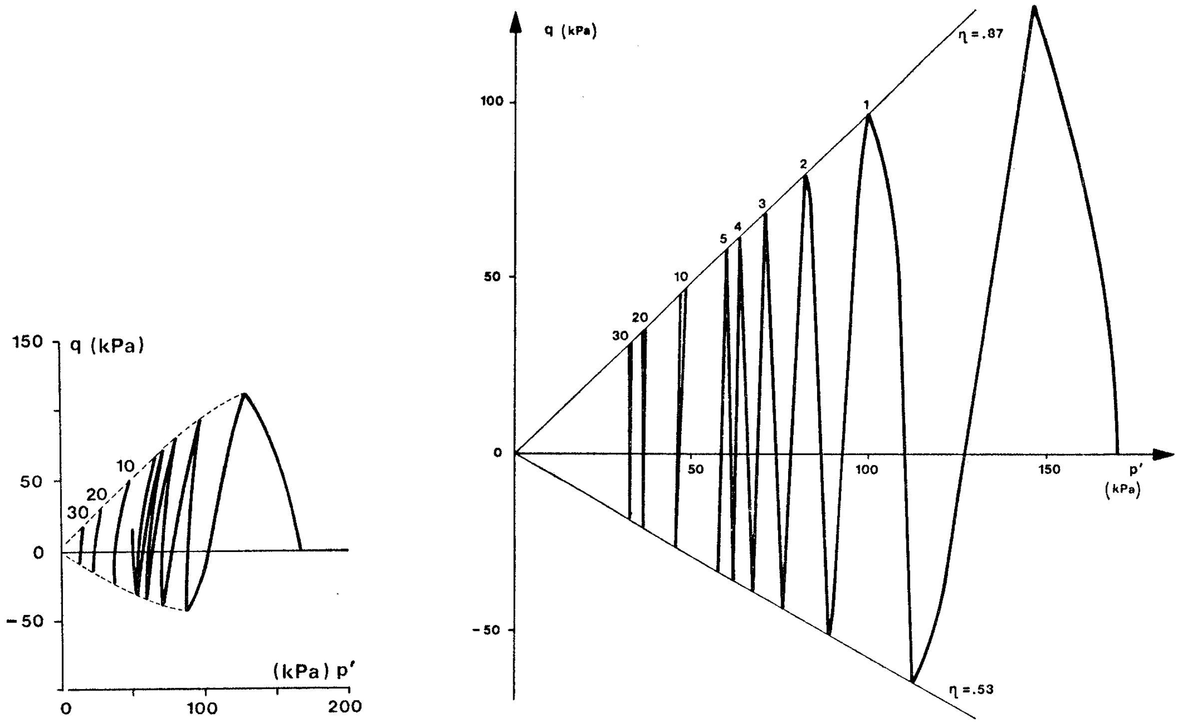

(a) (b)

Fig. 11. Calculated stress path for cyclic undrained test with constant shear strain amplitude-experimental data after Ishihara, Tatsuoka and Yasuda (1975) (a)

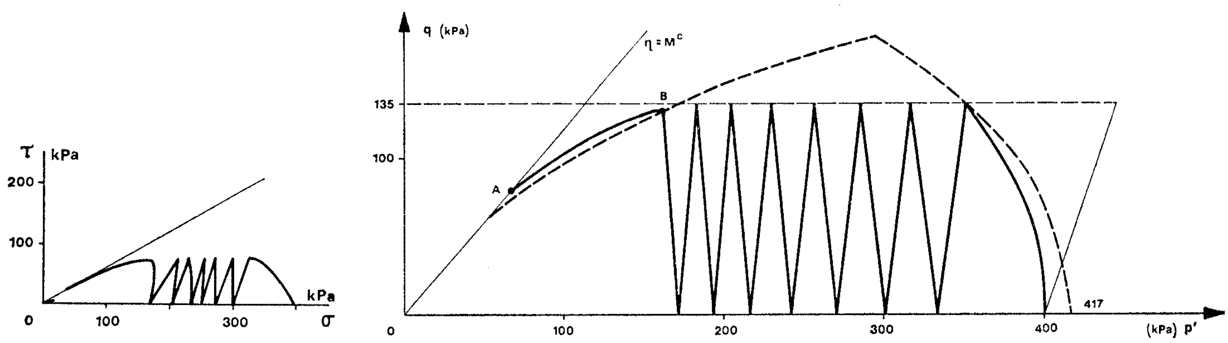

(a) (b)

Fig. 12. Calculated stress path in a cyclic undrained load controlled test on a loose sand with contractive structure-experimental data after Castro (1969) (a)

strength which drops to very low values for further loading, as experimentally observed.

CONCLUSIONS

Two kinds of behaviour of sands in undrained conditions are considered in this paper, one resulting from monotonic and the other from cyclic loading. Both lead to the same effect of liquefaction, although through completely different effective stress paths. It is possible however to describe both phenomena with the same mathematical model although in different ranges of its validity, sometimes combined.

Shear compaction and the eventuality of loop stabilization are effects which are taken into account by the model. The adopted way of describing cyclic shear compaction makes it possible to predict correctly the increase of the pore water pressure even for low values of the effective isotropic stress, which is not the case for some plasticity theories, as indicated recently by van Eekelen (1980). Moreover, it may be derived from the constitutive law that, depending on the material parameters, the number of cycles and the stress amplitude, a stabilization of the loop in undrained cyclic compression tests may or may not occur. This possibility has been experimentally shown by Sangrey (1967) on Newfield clay, which is a very silty clay. Therefore a qualitative prediction of a possible locus of stabilized loop maxima as a function of plastic strains may be constructed. Unfortunately, the scarcity of complete experimental data needed for the identification of this model, makes a quantitative study premature.

A substantial advantage of the model is the possibility of getting closed form solutions at least for portions of the stress strain relations and stress paths. This allows a simple identification of the values of constitutive parameters. Moreover their number is relatively low. Only three parameters in addition to those necessary to describe the elastic plastic behaviour are required to describe cyclic behaviour.

The model presented is limited to triaxial conditions but may be formally extended to cover more general loading conditions. However this goes beyond the intentions of the authors which merely endeavoured to clarify and to interpret the occurrence and interrelation of several aspects of liquefaction, as observed in experiments. It has been shown that such a goal may be achieved by modelling the behaviour of sand as elastic plastic in virgin loading and hysteretic within the current yield locus, with a suitable modification of a non-linear elastic constitutive law.

NOTATION

A_L=area of stress strain unloading-reloading loop
A_T=reference area of the loop
B_0, B=elastic and 'paraelastic' bulk moduli
D=dilatancy parameter
d=dilatancy
f=yield function
G=secant shear modulus
g=plastic potential
H=hardening modulus
h_0, h=sample height
L_0, L=elastic and 'paraelastic' shear moduli
$\mathcal{L}$=loading function
M=critical state stress ratio
m=yield function parameter
W=mass of loading device
p', q=stress invariants in triaxial plane
p'_c=preconsolidation pressure
p'_y, p'_g=abscissas of points on yield locus and plastic potential for $\eta=M$
q_P, q_R=stress deviator at peak and after liquefaction
R_D=damping ratio
v, ε=strain invariants in triaxial plane
y, z=constants
w=stress reversal locus
η=stress ratio
λ=isotropic compressibility
ξ, ξ^*=shear compaction parameters
μ=plastic potential parameter
χ, χ^e, χ^p=strain amplitude parameters

ψ'=hidden variable
ω_v, ω_s='paraelastic' parameters

REFERENCES

1) Casagrande, A. (1975) : "Liquefaction and cyclic deformation of sands, A critical review," Harvard SM Series No. 88 presented at 5th Pan. Am. Conf. SMFE, Buenos Aires.
2) Castro, G. (1969) : "Liquefaction of sand," Harvard SM Series No. 81.
3) Castro, G. (1975) : "Liquefaction and cyclic mobility of Saturated Sands," Proc. ASCE-GED, 101, GT 6, pp. 551-569.
4) Hardin, B. O. and Drnevich, V. P. (1972) : "Shear modulus and damping in soils : Measurement and parameters effect," Proc. ASCE-SMFE, 98, pp. 603-624.
5) Hueckel, T. and Nova, R. (1979) : "Some hysteresis effects of the behaviour of geologic media," Int. J. of Solids and Structures, 15, pp. 625-642.
6) Ishihara, K., Tatsuoka, F. and Yasuda, S. (1975) : "Undrained deformation and liquefaction of sand under cyclic stresses," Soils and Foundations, Vol. 15, No. 1, pp. 29-44.
7) Mroz, Z. and Lind, N. L. (1975) : "Simplified therories of cyclic plasticity," Acta Mechanica, 22, pp. 131-152.
8) Nova, R. (1981) : "A constitutive model for soil under monotonic and cyclic loading," to appear in Soil Mechanics-Transient and Cyclic Loads (G. N. Pande and O. C. Zienkiewicz Editors).
9) Nova, R. and Hueckel, T. (1979) : "An engineering theory of soil behaviour in unloading and reloading," TR 3-79 ISTC, Milano, to appear on Meccanica.
10) Nova, R. and Hueckel, T. (1980) : "A 'geotechnical' stress variables approach to cyclic behaviour of soils," Int. Symp. on Soils under Cyclic and Transient Loading, Swansea, 1, pp. 301-314.
11) Nova, R. and Wood, D. M. (1979) : "A constitutive model for sand in triaxial compression," Int. J. Num. Anal. Meth. Geomech., 3, 3, pp. 255-278.
12) Roscoe, K. H. and Burland, J. B. (1968) : "Stress strain behaviour of wet clay," in 'Engineering Plasticity', Cambridge Univ. Press, pp. 535-609.
13) Sangrey, D. A. (1967) : "The behaviour of soils subjected to repeated loading," Ph. D. Thesis Cornell Univ. Ithaca.
14) Schofield, A. N. and Wroth, C. P. (1968) : Critical State Soil Mechanics, Wiley.
15) Tatsuoka, F. (1972) : "Shear tests in a triaxial apparatus, A fundamental study on the deformation of sand," Ph. D. Thesis, Univ. of Tokyo (in Japanese).
16) van Eekelen, H. A. M. (1980) : "Fatigue models for cyclic degradation of soils," Proc. Int. Symp. 'Soils under cyclic and transient loading' Swansea.

APPENDIX

It is possible to make a simple dynamic analysis of the post-peak behaviour of a sample which is undergoing liquefaction. We shall confine our consideration to actual liquefaction, although there is no difficulty to extend it to other cases. We shall assume that the load exerted on the sample in the apparatus is increased with a certain rate, always positive. Thus while the axial stress, and also the deviatoric stress, reach the peak value and then start to decrease, the external load remains practically constant. Therefore a difference occurs between the externally applied load (and consequently stress) and the intrinsic stress response of the material. Inertia forces then may arise in order to maintain the dynamic equilibrium. This is associated to an accelerated motion of the sample and of a part of the loading device. At the same time the sample undergoes a substantial increase in diameter, which tends to reduce the mentioned stress difference.

Let then σ_{1P} and σ_{1R} be the axial stresses at peak and after liquefaction. Since the vertical strain at peak is small, it may be disregarded and we may assume that the area of the sample is still the initial one, A_0. On the contrary after liquefaction

$$A=A_0/(1-\varepsilon_1) \tag{A 1}$$

where $\varepsilon_1=x/h_0$ is the axial strain, x is the vertical displacement, h_0 is the initial height of the sample. Thus the vertical dynamic equilibrium equation may be written as

$$\mathcal{W}\ddot{x}+\sigma_{1R}\frac{A_0}{1-x/h_0}=\sigma_{1P}A_0 \tag{A 2}$$

where $\mathcal{W}$ is the mass of the loading system. Putting $y=1-x/h_0$ and $\dot{y}=z$ it is possible to integrate (A 2) and get

$$t=\int_y^1\frac{dy}{((2\,\sigma_{1P}A_0/(\mathcal{W}h_0)\cdot(\sigma_{1R}/\sigma_{1P}\cdot\ln y-y+\mathcal{W}h_0/(\sigma_{1P}A_0)\cdot v_0{}^2+1))^{1/2}} \tag{A 3}$$

where v_0 is the initial velocity of the deformation process. The integration of (A 3) may be performed by expanding the integrand in series. For small values of x an approximate solution may be found by putting

$$\ln y=\ln(1-x/h_0)\simeq -x/h_0=y-1 \tag{A 4}$$

Putting $v_0=0$, we get

$$t=\left(2\frac{h_0\varepsilon_1\mathcal{W}}{A_0(\sigma_{1P}-\sigma_{1R})}\right)^{1/2} \tag{A 5}$$

Let q_P and q_R be the deviatoric stresses at peak and after liquefaction. Assuming that $\mathcal{W}$ is given by the axial load divided by the gravity acceleration g, Eq. (A 5) becomes, since $\sigma_{1P}-\sigma_{1R}=q_P-q_R$,

$$t=\left(\frac{2\,h_0\varepsilon_1}{(1-q_R/q_P)g}\right)^{1/2} \tag{A 6}$$

Castro (1969) reports that in a test on loose Banding sand a strain of 18% is reached passing from $q_P=186$ kPa to $q_R=24.3$ kPa in .18 sec. Eq. (A 6) predicts, for a sample height of $h_0=.089$ m, that is appropriate for this case, a time of .062 sec. The difference may be due to the simplifying assumptions introduced and particularly to the fact that friction has been neglected and that a sudden strength drop from q_P and q_R has been implicitly assumed instead of the smooth transition observed in experiments.

(Received December 15, 1980)